

Design of Density Functionals That Are Broadly Accurate for Thermochemistry, Thermochemical Kinetics, and Nonbonded Interactions

Yan Zhao and Donald G. Truhlar*

Department of Chemistry and Supercomputing Institute, University of Minnesota,
207 Pleasant Street Southeast, Minneapolis, Minnesota 55455-0431

Received: January 31, 2005; In Final Form: April 28, 2005

This paper develops two new hybrid meta exchange-correlation functionals for thermochemistry, thermochemical kinetics, and nonbonded interactions. The new functionals are called PW6B95 (6-parameter functional based on Perdew–Wang-91 exchange and Becke-95 correlation) and PWB6K (6-parameter functional for kinetics based on Perdew–Wang-91 exchange and Becke-95 correlation). The resulting methods were comparatively assessed against the MGAE109/3 main group atomization energy database, against the IP13/3 ionization potential database, against the EA13/3 electron affinity database, against the HTBH38/4 and NHTBH38/04 hydrogen-transfer and non-hydrogen-transfer barrier height databases, against the HB6/04 hydrogen bonding database, against the CT7/04 charge-transfer complex database, against the DI6/04 dipole interaction database, against the WI7/05 weak interaction database, and against the new PPS5/05 π – π stacking interaction database. From the assessment and comparison of methods, we draw the following conclusions, based on an analysis of mean unsigned errors: (i) The PW6B95, MPW1B95, B98, B97-1, and TPSS1KCIS methods give the best results for a combination of thermochemistry and nonbonded interactions. (ii) PWB6K, MPWB1K, BB1K, MPW1K, and MPW1B95 give the best results for a combination of thermochemical kinetics and nonbonded interactions. (iii) PWB6K outperforms the MP2 method for nonbonded interactions. (iv) PW6B95 gives errors for main group covalent bond energies that are only 0.41 kcal (as measured by mean unsigned error per bond (MUEPB) for the MGAE109 database), as compared to 0.56 kcal/mol for the second best method and 0.92 kcal/mol for B3LYP.

1. Introduction

Development of exchange and correlation functionals for density functional theory (DFT) is an active research area in theoretical chemistry and physics.^{1–50} There are two different philosophies for developing new functionals, namely, nonempirical and semiempirical. The nonempirical approach is to construct functionals from first principles and subject to known exact constraints. DFT methods constructed this way may be called “ab initio” DFT methods. This approach has produced the successful PBE¹¹ and TPSS^{38,39,41} functionals.

However, the most popular DFT method in chemistry, B3LYP,^{8,9} has been constructed by the semiempirical approach. This involves choosing a flexible functional form depending on one or more parameters, and then fitting these parameters to a set of experimental data. B3LYP,^{8,9} B97-2,³⁰ VSXC,¹⁶ MPW1K,²⁵ MPWB1K,⁴⁴ and MPW1B95⁴⁴ are examples of functionals determined by the semiempirical approach.

Both the nonempirical and semiempirical DFT methods can be assigned to various rungs of “Jacob’s ladder”,²⁸ according to the number and kind of the ingredients in the functional. The lowest rung is the local spin density approximation (LSDA, in which the density functional depends only on density), and the second rung is the generalized gradient approximation (GGA, in which the density functional depends on density and its reduced gradient). The third rung is meta GGA, in which the functional also depends kinetic energy density. The fourth rung is hyper GGA,²⁸ which employs some percentage of HF exchange. Unfortunately, there is no nonempirical hyper-GGA thus far. However, there are two kinds of DFT methods that

belong to the fourth rung of the Jacob’s ladder, and they are called hybrid GGA (a combination of GGA with Hartree–Fock exchange, for example, B3LYP, PBE0, and MPW1K) and hybrid meta GGA (a combination of meta GGA with Hartree–Fock exchange, for example, MPWB1K, MPW1B95, and TPSSh). Both hybrid GGA and hybrid meta GGA are semiempirical, and they have been very successful for chemistry.

Recently we systematically tested a number of DFT methods against databases of atomization energies,^{42,44} barrier heights,^{42,44,49} and binding energies of nonbonded complexes.^{44,50} We found that MPW1B95 is one of best general-purpose DFT methods, and it gives excellent performance for nonbonded interactions. We also found that MPWB1K is the best DFT method for thermochemical kinetics and nonbonded interactions. Both MPW1B95 and MPWB1K are examples of hybrid meta GGAs, and both were parametrized within the past year.⁵¹

In the present study, we will further improve the MPW1B95 and MPWB1K methods by the semiempirical fitting approach. Because one of our goals is to develop a density functional that is simultaneously accurate for bond energies, barrier heights, and nonbonded interactions, including nonbonded interactions dominated by dispersion, and because DFT is often stated to be inappropriate for dispersion interactions, we distinguish two general approaches to improving DFT for dispersion interactions. In the first, which we will call empirical van der Waals correction methods,^{52,53} one adds explicit r^{-6} terms to DFT (where r is an interatomic distance). In such methods, one needs to develop different parameters for different atoms and in some cases even for different hybridization states.⁵² Furthermore, the

performance of empirical van der Waals correction methods for covalent interactions and for other types of nonbonded interaction such as charge-transfer interaction has not been evaluated. In the second general approach, one attempts to improve the performance of DFT for nonbonded interactions by improving the density functionals in the more traditional way. This, however, has proved to be difficult. For example, Walsh⁵⁴ has recently shown that two newly developed functionals, X3LYP⁴⁰ and xPBE,⁴⁷ are not capable of describing the interactions in methane dimers, benzene dimers, or nucleobase pair stacking, although both functionals were designed partly for nonbonded interactions. Walsh also showed that combining HF exchange with the Wilson-Levy correlation (HF + WL) approach⁵⁴ can give good predictions for van der Waals systems, but it would be expected that the HF + WL approach cannot give satisfactory results for covalent interactions because of the unbalanced exchange and correlation. Our goal here is to design some functionals that can perform equally well for both covalent interactions and for all types of nonbonded interactions. We optimize two new functionals, namely, PW6B95 and PWB6K, against a database of atomization energies, barrier heights, a hydrogen bond energy, and the dissociation energy of a nonpolar van der Waals complex. To test our functionals, we examine their performance for hydrogen bonding, charge-transfer interactions, dipole interactions, weak interactions, and π - π stacking interactions. We compare the performance of the newly developed functionals to that of LSDA, GGA, meta GGA, and hybrid GGA functionals and previous hybrid meta GGA methods.

Hybrid density functionals are less accurate for systems requiring a multi-configuration zero-order description (systems with so-called “multireference character”). The functionals studied here do not overcome that problem and are designed for use on problems where the admixture of single-configuration Hartree-Fock exchange is not inappropriate.

Section 2 presents our training sets and test sets. Section 3 discusses the theory and parametrization of the new methods. Section 4 presents results and discussion.

2. Databases

2.1. Binding8. The training set for the PW6B95 model is the Binding8 database, which includes the six atomization energies in the AE6 representative database presented previously⁵⁵ and the binding energies of (H₂O)₂ dimer and (CH₄)₂ dimer. The AE6 set of atomization energies consists of SiH₄, S₂, SiO, C₃H₄ (propyne), C₂H₂O₂ (glyoxal) and C₄H₈ (cyclobutane). We have previously used AE6 as a training set to optimize the MPW1B95,⁴⁴ TPSS1KCIS,⁴⁸ and MPW1KCIS⁴⁹ methods. The Binding8 database is given in the Supporting Information.

2.2. Kinetics9. To parametrize the PWB6K model, we also used (in addition to Binding8) a database of 3 forward barrier heights, 3 reverse barrier heights, and 3 energies of reaction for the three reactions in the BH6⁵⁵ database; this 9-component database is called Kinetics9. We have previously used this training set to optimize the BB1K,⁴³ MPWB1K⁴⁴ and MPWKICIS1K⁴⁹ methods. The Kinetics9 database is also given in the Supporting Information.

2.3. MGAE109 Test Set. The MGAE109 test set consists of 109 atomization energies (AEs). This AE test set contains a diverse set of molecules including organic and inorganic compounds (but no transition metals; the MG in the name of this database denotes main group elements, and AE denotes atomization energies). All 109 data are pure electronic energies; i.e., zero-point energies and thermal vibrational-rotational

energies have been removed by methods discussed previously.^{48,56,57} The 109 zero-point-exclusive atomization energies are part of Database/3⁵⁷ and have been updated⁴⁸ recently. The updates include NO, CCH, C₂F₄, and singlet and triplet CH₂, the updated database is called MGAE109/05, and it is a subset of Database/4.

2.4. Ionization Potential and Electron Affinity Test Set. The zero-point-exclusive ionization potential (IP) and electron affinity (EA) test set is taken from a previous paper.⁵⁶ This data set is also part of Database/3, and it consists of six atoms and seven molecules for which the IP and EA are both present in the G3⁵⁸ data set. These databases are called IP13/3 and EA13/3, respectively.

2.5. HTBH38/04 Database. The HTBH38/04 database consists of 38 transition state barrier heights for hydrogen transfer (HT) reactions, and it is taken from previous papers.^{48,49} It consists of 38 transition state barrier heights of hydrogen transfer reactions, and the HTBH38/04 database is listed in the Supporting Information.

2.6. NHTBH38/04 Database. The HTBH38/04 database consists of 38 transition state barrier heights for non-hydrogen-transfer (NHT) reactions, and it is taken from a previous paper.⁴⁹ This test set consists of 12 barrier heights for heavy-atom transfer reactions, 16 barrier heights for nucleophilic substitution (NS) reactions, and 10 barrier heights for non-NS unimolecular and association reactions.

2.7. HB6/04 Database. The hydrogen bond database consists of the equilibrium binding energies of six hydrogen bonding dimers, namely, (NH₃)₂, (HF)₂, (H₂O)₂, NH₃⋯H₂O, (HCONH₂)₂, and (HCOOH)₂. This database is taken from a previous paper,⁵⁰ and it is listed in the Supporting Information.

2.8. CT7/04 Database. The charge transfer (CT) database consists of binding energies of seven charge-transfer complexes, in particular C₂H₄⋯F₂, NH₃⋯F₂, C₂H₂⋯ClF, HCN⋯ClF, NH₃⋯Cl₂, H₂O⋯ClF, and NH₃⋯ClF. This database is taken from a previous paper,⁵⁰ and it is also listed in the Supporting Information.

2.9. DI6/04 Database. The dipole interaction (DI) database consists of binding energies of six dipole interaction complexes: (H₂S)₂, (HCl)₂, HCl⋯H₂S, CH₃Cl⋯HCl, CH₃SH⋯HCN, and CH₃SH⋯HCl. This database is taken from a previous paper,⁵⁰ and it is also listed in the Supporting Information.

2.10. WI7/05 Database. The weak interaction database consists of binding energies of seven weak interaction complexes, namely, HeNe, HeAr, Ne₂, NeAr, CH₄⋯Ne, C₆H₆⋯Ne, and (CH₄)₂, all of which are bound by dispersion interactions. The four rare gas dimers in the WI7/05 database represent dispersion interactions that are expected to be typical interaction of hydrogen—first row, first row—first row, hydrogen—second row, and first row — second row elements, respectively. This database is a subset of a previous WI9/04 database,⁵⁰ and it is also listed in the Supporting Information.

2.11. PPS5/05 Database. The π - π stacking (PPS) database consists of binding energies of five π - π stacking complexes, namely, (C₂H₂)₂, (C₂H₄)₂, sandwich (C₆H₆)₂, T-shaped (C₆H₆)₂, and parallel-displaced (C₆H₆)₂. This database is listed in Table 1. The best estimate of the binding energies of (C₂H₂)₂ and (C₂H₄)₂ are obtained by W1⁵⁹ calculations performed for the present article by methods explained in a previous paper.⁵⁰ The best estimate of binding energies of sandwich (C₆H₆)₂, T-shaped (C₆H₆)₂, and parallel-displaced (C₆H₆)₂ are taken from the paper of Sinnokrot et al.⁶⁰

2.12. Database Availability. All above-mentioned databases are also available at the Truhlar group website.⁶¹

TABLE 1: Binding Energies (kcal/mol) in the π - π Stacking Database (PPS5/05)

complexes	best estimate	ref
(C ₂ H ₂) ₂	1.34	50
(C ₂ H ₄) ₂	1.42	50
Sandwich (C ₆ H ₆) ₂	1.81	60
T-shaped (C ₆ H ₆) ₂	2.74	60
parallel-displaced (C ₆ H ₆) ₂	2.78	60
average	2.02	

3. Computation Methods, Theory and Parametrization

3.1. Geometries, Basis Sets, and Spin–Orbit Energy. All calculations for the AE6, MGAE109, IP13/3, EA13/3, HTBH38/04 and NHTBH38/04 databases are single-point calculations at QCISD/MG3 geometries, where QCISD is quadratic configuration interaction with single and double excitations,⁶² and MG3 is the modified^{63,64} G3Large⁵⁸ basis set. The MG3 basis set,⁶³ also called G3LargeMP2,⁶⁴ is the same as 6-311++G(3d2f, 2df, 2p)^{65,66} for H–Si, but improved⁵⁸ for P–Ar. The QCISD/MG3 geometries for molecules and saddle points in the MGAE109, IP13/3, EA13/3, HTBH38/04 and NHTBH38/04 databases can be obtained from the Truhlar group database website.⁶¹

Geometries for all molecules in the nonbonded database (HB6/04, CT7/04, DI6/04, and WI7/05) are optimized at the MC-QCISD/3 level, where MC-QCISD is the multi-coefficient QCISD method,^{57,67} which is one of the most cost-efficient methods of the set of multi-coefficient correlation methods (MCCMs). The geometries for the benzene dimers in the PPS5/05 database are taken from Sinnokrot and Sherrill.⁶⁸ The geometries for all monomers and complexes in the HB6/04, CT7/04, DI6/04, WI7/05, and PPS5/05 databases can be obtained from the Truhlar group database website.⁶¹

We tested all DFT methods with the MG3S basis sets. The MG3S basis⁵⁶ is the same as MG3 except it omits diffuse functions on hydrogens. However, the optimization of new parameters in density functionals are carried out with the 6-31+G(d,p)⁶⁶ basis set (also called DIDZ).

In all of the calculations presented in this paper, the spin–orbit stabilization energy was added to atoms and open-shell molecules for which it is nonzero, as described previously.⁶³

3.2. Counterpoise Corrections and Software. For non-bonded complexes, we perform calculations with and without the counterpoise corrections^{69,70} for basis set superposition error (BSSE). All calculations were performed with a locally modified *Gaussian03* program⁷¹ and use the ultrafine grid for evaluating integrals over density functionals.

3.3. Theory. **3.3.1. Exchange Functional.** The LSDA exchange energy can be written as

$$E_X^{\text{LSDA}} = A_x \sum_{\sigma} \int \rho_{\sigma}(\mathbf{r})^{4/3} d\mathbf{r} \quad (1)$$

where ρ_{σ} is the density of electrons with spin σ (where $\sigma = \alpha$ or β , and ρ_{σ} is also called spin density), and the constant A_x in eq 1 is defined as

$$A_x = -\frac{3}{2} \left(\frac{3}{4\pi} \right)^{1/3} \quad (2)$$

The GGA exchange energy can be expressed as

$$E_X^{\text{GGA}} = E_X^{\text{LSDA}} - \sum_{\sigma} \int F^{\text{GCE}}[x_{\sigma}] \rho_{\sigma}(\mathbf{r})^{4/3} d\mathbf{r} \quad (3)$$

where reduced gradient of the density with spin σ is

$$x_{\sigma} = \frac{|\nabla \rho_{\sigma}|}{(\rho_{\sigma})^{4/3}} \quad (4)$$

$F^{\text{GCE}}[x_{\sigma}]$ is the gradient-corrected enhancement factor. The gradient-corrected enhancement factor for the PW91⁵ and mPW¹⁴ exchange functional is

$$F^{\text{GCE}}[x_{\sigma}] = \frac{bx_{\sigma}^2 - (b - \beta)x_{\sigma}^2 \exp(-cx_{\sigma}^2) - 10^{-6}x_{\sigma}^d}{1 + 6bx_{\sigma} \sinh^{-1}x_{\sigma} - \frac{10^{-6}x_{\sigma}^d}{A_x}} \quad (5)$$

where $\beta = 5(36\pi)^{-5/3}$ and $c = 1.6455$ in both functionals. In the PW91 functional, $b = 0.0042$ and $d = 4$, whereas in the mPW functional, $b = 0.00426$ and $d = 3.72$. Note that in the original mPW paper,¹⁴ the value of parameters b and d were incorrectly tabulated as 0.0046 and 3.73.

3.3.2. Correlation Functional. In the present study, we use Perdew and Wang’s functional⁶ for the correlation part of the LSDA. Then, following the analysis of Stoll, Pavlidou, and Preuss,⁷² one can decompose the LSDA correlation energy into opposite-spin (opp) and parallel-spin ($\sigma\sigma$) correlation energy components for the uniform electron gas (UEG):

$$E_{\text{Copp}}^{\text{UEG}}(\rho_{\alpha}, \rho_{\beta}) = E_C^{\text{LSDA}}(\rho_{\alpha}, \rho_{\beta}) - E_C^{\text{LSDA}}(\rho_{\alpha}, 0) - E_C^{\text{LSDA}}(0, \rho_{\beta}) \quad (6)$$

$$E_{\text{C}\sigma\sigma}^{\text{UEG}}(\rho_{\sigma}) = E_C^{\text{LSDA}}(\rho_{\sigma}, 0) \quad (7)$$

where $E_C^{\text{LSDA}}(\rho_{\alpha}, \rho_{\beta})$ is the LSDA correlation energy.

Note that eq 7 does not vanish in the one-electron case, and this nonvanishing is a manifestation of self-interaction error. To correct this self-interaction error, Becke¹⁰ used a quantity, D_{σ} , which is defined as

$$D_{\sigma} = 2\tau_{\sigma} - \frac{1}{4} \frac{|\nabla \rho_{\sigma}|^2}{\rho_{\sigma}} \quad (8a)$$

and

$$\tau_{\sigma} = \frac{1}{2} \sum_i^{\text{occup}} |\nabla \Psi_{i\sigma}|^2 \quad (8b)$$

where τ_{σ} is the kinetic energy density of electrons with spin σ , defined in terms of the occupied Kohn–Sham orbitals $\Psi_{i\sigma}$. D_{σ} can be also written as

$$D_{\sigma} = 2(\tau_{\sigma} - \tau_{\sigma}^{\text{W}}) \quad (9a)$$

where

$$\tau_{\sigma}^{\text{W}} = \frac{1}{8} \frac{|\nabla \rho_{\sigma}|^2}{\rho_{\sigma}} \quad (9b)$$

and τ_{σ}^{W} is the von Weizsäcker kinetic energy density.⁷³ In one-electron case, $\tau_{\sigma} = \tau_{\sigma}^{\text{W}}$, so D_{σ} vanishes in any one-electron system. Becke used D_{σ} as a self-interaction correction factor in the parallel spin case. Note that the uniform electron gas limit ($\nabla \rho_{\sigma} \rightarrow 0$) of D_{σ} is

$$D_{\sigma}^{\text{UEG}} = \frac{3}{5} (6\pi^2)^{2/3} \rho_{\sigma}^{5/3} \quad (10)$$

Now we can write down the B95 correlation functional¹⁰ by

incorporating the gradient correction factors for the opposite spin and parallel spin case, and incorporating the self-interaction correction factor for the parallel spin case.

The opposite-spins correlation energy of the B95 functional can be expressed as

$$E_C^{\text{opp}} = [1 + c_{\text{opp}}(x_\alpha^2 + x_\beta^2)]^{-1} E_{C_{\text{opp}}}^{\text{UEG}} \quad (11)$$

and for parallel spins,

$$E_C^{\sigma\sigma} = [1 + c_{\sigma\sigma} x_\sigma^2]^{-2} \frac{D_\sigma}{D_{\text{UEG}}} E_{C_{\sigma\sigma}}^{\text{UEG}} \quad (12)$$

The total correlation energy is given by

$$E_C = E_C^{\text{opp}} + E_C^{\alpha\alpha} + E_C^{\beta\beta} \quad (13)$$

Becke fitted the parameters c_{opp} and $c_{\sigma\sigma}$ in eq 11 and eq 12 to the correlation energies of the helium (c_{opp}) and the neon ($c_{\sigma\sigma}$) atoms. The values of these two parameters in the B95 functional are

$$c_{\text{opp}} = 0.0031 \quad c_{\sigma\sigma} = 0.038 \quad (14)$$

3.3.3. Hybrid Meta Functional. The one-parameter hybrid Fock-Kohn–Sham operator can be written as follows:^{10,25}

$$F = F^{\text{H}} + (X/100)F^{\text{HFE}} + [1 - (X/100)](F^{\text{SE}} + F^{\text{GCE}}) + F^{\text{C}} \quad (15)$$

where F^{H} is the Hartree operator (i.e., the nonexchange part of the Hartree–Fock operator), F^{HFE} is the Hartree–Fock exchange operator, X is the percentage of Hartree–Fock exchange, F^{SE} is the Slater local density functional (also called Dirac–Slater) for exchange,^{74,75} F^{GCE} is the gradient correction for the exchange functional, and F^{C} is the total correlation functional including both local and gradient-corrected parts and a dependence on kinetic energy density. In the MPW1B95 and MPWB1K models,⁵¹ we used the mPW exchange functional¹⁴ (eq 5) for F^{GCE} and the Becke95¹⁰ functional (eqs 11–13) for F^{C} .

3.4. Optimization of the New Hybrid Meta Functionals.

All parameter optimizations were carried out with a genetic algorithm. We optimize two new methods using different training functions. In both new methods, we optimize the b , c , and d parameters in PW exchange functional (eq 5), the c_{opp} and $c_{\sigma\sigma}$ parameters in the Becke95 correlation functional, and the percentage, X , of Hartree–Fock exchange. We minimize these parameters in a self-consistent way by solving the Fock-Kohn–Sham equation using the DIDZ basis set with QCISD/MG3 geometries for the molecules in the AE6 database, and with MC-QCISD/3 geometries for $(\text{H}_2\text{O})_2$ and $(\text{CH}_4)_2$. We also turned on counterpoise correction⁶⁹ (cp) to correct basis set superposition error (BSSE) during the optimization for $(\text{H}_2\text{O})_2$ and $(\text{CH}_4)_2$ dimers.

For the first new functional, we optimized the parameters against the Binding8 database to minimize the following training function:

$$F_3 = \text{MUEPB}(\text{AE6}) + 3 \times \text{MUE}(D_c[(\text{H}_2\text{O})_2], D_c[(\text{CH}_4)_2]) \quad (16)$$

where MUEPB is the mean unsigned error (MUE, same as mean absolute deviation (MAD)) per bond. In particular, MUEPB is obtained by dividing the MUE for AE6 database by the average

TABLE 2: Parameters in the MPW1B95 and MPWB1K Methods and in the New Functionals

method	exchange			correlation		X
	b	c	d	c_{opp}	$c_{\sigma\sigma}$	
MPW1B95	0.00426 ^a	1.6455 ^b	3.7200 ^a	0.00310 ^c	0.03800 ^c	31 ^d
MPWB1K	0.00426 ^a	1.6455 ^b	3.7200 ^a	0.00310 ^c	0.03800 ^c	44 ^d
PWB6K	0.00539	1.7077	4.0876	0.00353	0.04120	46 ^e
PW6B95	0.00538	1.7382	3.8901	0.00262	0.03668	28

^a Same as mPW (ref 14). ^b Same as PW91 (ref 5). ^c Same as Becke95 (ref 10). ^d Reference 51. ^e In the PWB6K functional, $X = 31$ at the end of the first stage. Then all other parameters are frozen, and X is re-optimized for kinetics.

number of bonds per molecule in this database. The second term of eq 16 is the MUE for the equilibrium binding energies of $(\text{H}_2\text{O})_2$ and $(\text{CH}_4)_2$ with a weight of 3, because these numbers are much smaller than the bond energies in AE6. The functional optimized in this way is called PW6B95, which denotes (in the usual way) a 6-parameters functional based on PW91 exchange and Becke95 correlation.

For the second new functional, the parameters were optimized in two stages. First we optimized all six parameters against the training function F_6 , which is the same as F_3 , except that the MUE in the $(\text{H}_2\text{O})_2$ and $(\text{CH}_4)_2$ binding energies is weighted by 6 instead of 3. Then we froze the b , c , d , c_{opp} , and $c_{\sigma\sigma}$ parameters, and we reoptimized X against the Kinetics9 database. In particular, X was adjusted to minimize the root-mean-square-error (RMSE) for the Kinetics9 database. This second functional is called PWB6K, which denotes a functional based on PW91 exchange and Becke95 correlation, with 6 parameters optimized to improve nonbonded interactions and kinetics (K).

All optimized parameters are listed in Table 2, where they are compared to the parameters in MPW1B95 and MPWB1K.

For plotting, we define a total GGA enhancement factor F^{GGA} as

$$F^{\text{GGA}}[s] = F^{\text{GCE}}[s] + 1 \quad (17)$$

where $F^{\text{GCE}}[s]$ is the factor in eq 3. In addition, we use another definition of reduced gradient, in particular

$$s = \frac{|\nabla\rho|}{(24\pi^2)^{1/3} \rho^{4/3}} \quad (18)$$

Thus, for a closed-shell system with $\rho = 2\rho_\sigma$, we have $s = (48\pi^2)^{-1/3} x_\sigma$. The total enhancement factors for the B, mPW, PW91, and X exchange functionals and for the exchange parts of the PW6B95 and PWB6K methods are plotted in Figure 1. Interestingly, the shape of the exchange part of PWB6K is close to that for PW91 exchange, whereas the PW6B95 exchange lies between mPW and PW91 when $s > 4$. This may be surprising at first, but one should remember that one cannot evaluate exchange functionals separately from the correlation ones, to which they are added.

3.5. Assessment of the New Hybrid Meta Functionals. We fitted our new functionals against a very small data set (8 data in Binding8, 9 data in Kinetics9), but we assess the new functionals against a much larger data set that includes 109 atomization energies (MGAE109), 13 ionization potentials (IP13), 13 electron affinities (EA13), 76 barrier heights (HT-BH38 and NHTBH38), 6 hydrogen dimers (HB6), 7 charge-transfer complexes (CT7), 6 dipole interaction complexes (DI6), 7 weak interaction complexes (WI7), and 5 π - π stacking complexes (PPS5). We compare the new methods to a LSDA,

TABLE 3: Summary of the DFT Methods Tested

method	X^a	year	type	ex functional ^b corr functional ^c	ref
SPWL	0	1992	LSDA	Slater's local ex Perdew–Wang local	6, 76
B3LYP	20	1994	hybrid GGA	Becke88 Lee–Yang–Parr	3, 4, 9
B1B95	25	1996	hybrid meta GGA	Becke88 Becke95	3, 10
PBE	0	1996	hybrid GGA	PBE ex PBE corr	11
PBE1PBE ^d	25	1996	hybrid GGA	PBE ex PBE corr	11
mPW1PW91 ^e	25	1998	hybrid GGA	modified PW91 Perdew–Wang91	5, 14
B97-1	21	1998	hybrid GGA	B97-1 ex B97-1 corr	17
B98	21.98	1998	hybrid GGA	B98 ex B98 corr	15
MPW1K	42.8	2000	hybrid GGA	modified PW91 Perdew–Wang91	14, 24
B97-2	21	2001	hybrid GGA	B97-2 ex B97-2 corr	17
TPSS	0	2003	meta GGA	TPSS ex TPSS corr	38, 39
TPSSh	10	2003	hybrid meta GGA	TPSS ex TPSS corr	38, 39
X3LYP	21.8	2004	hybrid GGA	Becke88+PW91 Lee–Yang–Parr	3, 4, 5, 40
MPW3LYP	21	2004	hybrid GGA	modified PW91 Lee–Yang–Parr	4, 14, 51
TPSSKCIS	0	2004	hybrid meta GGA	TPSS ex KCIS corr	20, 21, 34, 38, 39
BB1K	42	2004	hybrid meta GGA	Becke88 Becke95	3, 10, 43
MPW1B95	31	2004	hybrid meta GGA	modified PW91 Becke95	10, 14, 51
MPWB1K	44	2004	hybrid meta GGA	modified PW91 Becke95	10, 14, 51
TPSS1KCIS	13	2004	hybrid meta GGA	TPSS ex KCIS corr	20, 21, 34, 38, 39, 43
MPW1KCIS	15	2004	hybrid meta GGA	modified PW91 KCIS corr	10, 20,21,34,49
MPWKCIS1K	41	2004	hybrid meta GGA	modified PW91 KCIS corr	10, 20,21,34,49
PBE1KCIS	22	2005	hybrid meta GGA	PBE ex KCIS corr	11, 20, 21, 34, 50
PW6B95	28	2005	hybrid meta GGA	PW6B95 ex PW6B95 corr	this work
PWB6K	46	2005	hybrid meta GGA	PWB6K ex PWB6K corr	this work

^a X denotes the percentage of HF exchange in the functional. ^b Upper entry. ^c Lower entry. ^d Also called PBE0. ^e Also called mPW1PW, mPW0, and MPW25.

namely, Slater exchange⁷⁶ plus Perdew–Wang⁶ local correlation (SPWL), and to a GGA: namely, PBE.¹¹ We also compare the new methods to two meta-GGA methods (TPSS^{38,39} and TPSSKCIS^{20,21,34,38,39}) and to eight hybrid GGA methods: B3LYP,^{4,8,9} B97-1,¹⁷ B97-2,³⁰ mPW1PW91,¹⁴ MPW1K,²⁵ MPW3LYP,^{4,14,51} PBE1PBE,¹¹ and X3LYP.⁴⁰ We also compare the new functionals to nine hybrid meta GGA methods, B1B95,¹⁰ BB1K,⁴³ MPW1B95,⁵¹ MPWB1K,⁵¹ MPW1KCIS,⁴⁹ MPWKCIS1K,⁴⁹ PBE1KCIS,⁵⁰ TPSS1KCIS,^{20,21,34,38,39,43} and TPSSh,^{38,39} and to an ab initio wave function method, MP2.⁷⁷ All DFT methods in the present paper are listed in the Table 3 in the chronological order of their invention.

4. Results and Discussion

In this section we will gauge the quality of the results by mean unsigned errors (MUEs), which are the averages of the absolute deviations of calculated values from database values, and by mean signed errors (MSE), which are used to detect systematic deviations. However, for atomization energies we use MUE per bond (MUEPB) and MSE per bond (MSEPB)

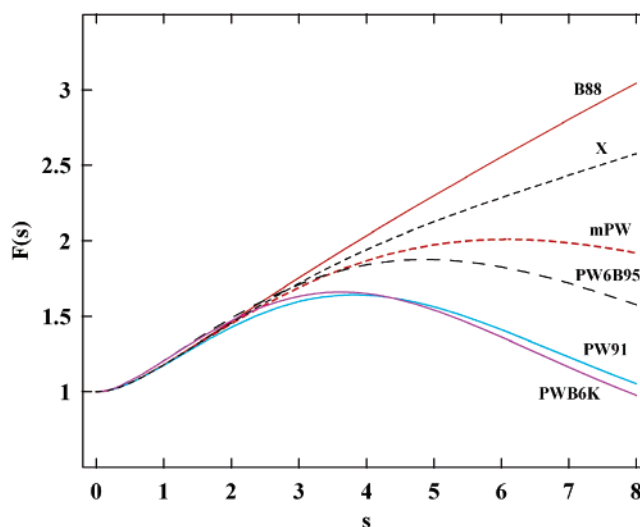


Figure 1. GGA enhancement factors for the Becke88, mPW, PW91, PW6B95, PWB6K, and X exchange functionals.

TABLE 4: Mean Errors^a (kcal/mol for Ionization Potentials (IP) and Electron Affinities (EA) and kcal/mol per Bond for Atomization Energies (AE))^b

method	MGAE109		IP13		EA13		TMUE
	MSEPB	MUEPB	MSE	MUE	MSE	MUE	
PW6B95	-0.02	0.40	2.24	3.24	0.72	1.78	0.81
B1B95	-0.23	0.55	-0.13	2.18	3.02	3.16	0.96
MPW1B95	0.31	0.62	0.36	2.14	2.72	2.91	0.98
B98	-0.50	0.64	1.99	3.21	0.30	1.84	1.00
B97-2	-0.20	0.65	0.46	2.21	2.41	2.89	1.02
TPSS1KCIS	-0.05	0.67	0.91	2.63	1.84	2.81	1.07
B97-1	-0.39	0.75	0.99	2.84	1.09	2.02	1.07
MPW3LYP	-0.19	0.63	2.72	4.32	-0.70	2.14	1.13
PBE1PBE	0.11	0.91	2.44	3.23	1.50	2.76	1.31
mPW1PW91	-0.73	0.88	3.17	3.72	1.09	2.62	1.32
TPSS	0.63	1.03	1.80	3.11	0.51	2.31	1.36
MPW1KCIS	-0.24	0.68	5.04	5.46	-2.59	2.76	1.34
PBE1KCIS	-0.05	0.79	4.77	5.08	-1.84	2.39	1.36
TPSSh	-0.12	0.98	1.96	3.17	1.40	2.81	1.37
MPWB1K	-0.84	0.98	0.51	2.05	3.99	4.11	1.38
TPSSKCIS	0.91	1.13	0.72	2.78	0.64	2.21	1.40
B3LYP	-0.69	0.91	3.58	4.72	-1.51	2.29	1.41
BB1K	-1.32	1.34	0.13	2.09	4.28	4.36	1.70
PWB6K	-1.41	1.43	1.57	2.28	3.23	3.59	1.72
X3LYP	-1.26	1.42	2.58	4.73	-0.41	3.04	1.89
BLYP	-0.47	1.49	-0.41	4.87	-0.11	2.63	1.93
MP2	-1.11	2.04	-3.57	3.57	2.92	2.99	2.28
MPW1K	-2.33	2.34	3.41	3.53	2.79	3.71	2.59
MPWKCIS1K	-2.63	2.67	5.32	5.32	0.05	2.61	2.92
PBE	2.80	3.03	2.11	3.58	-1.20	2.22	3.01
SPWL	16.89	16.89	4.34	5.18	-5.77	5.80	14.70

^aMUEPB denotes mean unsigned error (MUE) per bond. MSE denotes mean signed error. TMUE denotes total MUE and it is defined as: $TMUE = [MUEPB \times 109 + MUE(IP) \times 13 + MUE(AE) \times 13] / 135$. ^bQCISD/MG3 geometries and the MG3S basis set are used for calculations in this table.

because this allows^{42,43} more transferable comparison between databases with different average sizes of molecules. To make the trends more clear, in every table we will list the methods in increasing order of the values in the key (overall) error column, which is always the last column of a given table. The five smallest average errors for each of the individual databases and the 10 smallest average errors overall (for each table) are in bold.

4.1. Thermochemistry: AE, IP, and EA Results. Table 4 summarizes the errors in AEs, IPs, and EAs for all tested methods. Table 4 shows that the PW6B95, B1B95, MPW1B95, MPW3LYP methods give the best results for AE calculations. PW6B95 is the only method which has MUEPB less than 0.5 kcal/mol. Note that the second best method for atomization energy has an error much larger, in fact 37% larger, than PW6B95, and the most popular method B3LYP has an error 124% larger than PW6B95.

MPWB1K, BB1K, MPW1B95, and B1B95 have the best performance for IP calculations, whereas PW6B95, B97-1, TPSSKCIS, and PBE give the best performance for EA calculations. The outstanding performance of PW6B95 for electron affinities is particularly noteworthy because no electron affinity data were used in the parametrization.

To compare their performance for thermochemistry, we defined the TMUE (total MUE) as follows:

$$TMUE = [MUEPB(AE) \times 109 + MUE(IP) \times 13 + MUE(EA) \times 13] / 135 \quad (19)$$

If we use TMUE as a criterion for thermochemistry, Table 4 shows that PW6B95 is the best functional, followed by B1B95, MPW1B95, and B98. A final choice of method for many applications should probably be based on a broader assessment

with more diverse data than on small differences between the higher-quality methods in Table 4, and one of the goals of the rest of this paper is to present such an assessment.

Before moving on though, it is important to emphasize that PW6B95 is parametrized only against the Binding8 data set. Even though the new functional is parametrized on this small data set, it shows good performance for the much larger MGAE109/3 database and for the IP and EA databases.

Both new methods, and in fact most of the DFT methods tested, outperform MP2 in terms of TMUE.

If we compare the nonempirical functionals on the first three rungs of Perdew's nonempirical Jacob's ladder^{28,35,39} for organizing DFT approximations, Table 3 shows that, as we climb the nonempirical ladder, the TMUE calculations improve significantly from LSDA (i.e., SPWL) to PBE (TMUE reduces from 14.7 to 3.0 kcal/mol) and also improve by more than a factor of 2 from PBE to TPSS (TMUE reduces from 3.0 to 1.4 kcal/mol).

4.2. Thermochemical Kinetics: HTBH38/04 and NHT-BH38/04 Results. Table 5 gives the mean errors for the HTBH38/04 and NHTBH38/04 databases with the MG3S basis set. We also tabulated a value of mean MUE (called MMUE) that is defined as $1/4$ times the MUE for heavy-atom transfer barrier heights plus $1/4$ times the MUE for S_N2 barrier heights plus $1/4$ times the MUE for unimolecular and association barrier heights plus $1/4$ times the MUE for hydrogen transfer barrier heights.

Table 5 shows that the BB1K, PWB6K, MPWB1K, and MPW1K methods give the best results for heavy-atom-transfer barrier height calculations. MP2, B1B95, PWB6K, and MPWKCIS1K have the best performance for nucleophilic substitution barrier height calculations. B1B95, MPW1B95, PW6B95, and BB1K give the best performance for non-NS unimolecular and association barrier height calculations. The BB1K, PWB6K, MPWB1K, and MPW1K methods give the best performance for hydrogen transfer barrier height calculations, and they also give the lowest values of MMUE, which means they give the best performance for overall barrier height calculation.

Another quantity, average MUE or AMUE, is defined as

$$AMUE = [MUEPB(\Delta E, 38) + MMUE(BH76)] / 2 \quad (20)$$

where $MUE(\Delta E, 38)$ is the mean unsigned error for the energy of reactions for the 38 reactions in the HTBH38 and NHTBH38 database. If we use AMUE as a criterion to justify the performance of a DFT method for thermochemical kinetics, Table 5 shows that BB1K, PWB6K, and MPWB1K are the best, followed by B1B95, MPW1K, and MPW1B95.

4.3. Nonbonded Interactions. The mean errors for non-bonded interaction are listed in Table 6 and Table 7. In both tables, we use "no-cp" to denote calculations without the counterpoise correction for the BSSE, and we use "cp" to denote calculations that do include the counterpoise correction for the BSSE. Table 6 summarizes MUEs, and Table 7 presents MSEs.

In Table 6, we only listed MUEs. We also defined a mean MUE:

$$MMUE = [MUE(no-cp) + MUE(cp)] / 2 \quad (21)$$

Although the cp correction has many advocates, it is often impractical to include this correction (for example, it is impractical for condensed-phase simulations and it is ambiguous for process involving bond making as well as nonbonded

TABLE 5: Mean Errors for HTBH38 and NHTBH38 Database^{a,b,c}

methods	heavy atom transfer (12)		NS ^d (16)		unimol and assoc ^e (10)		hydrogen transfer (38)		MMUE	AMUE
	MSE	MUE	MSE	MUE	MSE	MUE	MSE	MUE		
BB1K	-0.69	1.58	1.23	1.30	0.53	1.44	-0.57	1.16	1.37	1.50
PWB6K	-0.24	1.61	0.94	1.10	0.65	1.53	-0.50	1.28	1.38	1.59
MPWB1K	-0.77	1.69	1.08	1.19	0.52	1.61	-0.85	1.29	1.45	1.60
B1B95	-4.73	4.73	-0.95	1.08	-0.58	1.21	-2.80	2.80	2.45	1.78
MPW1K	-0.83	1.89	1.12	1.28	0.96	2.42	-0.60	1.32	1.73	1.82
MPW1B95	-4.62	4.62	-0.81	1.21	-0.52	1.31	-3.02	3.02	2.54	1.92
MPWKICIS1K	-0.77	1.97	0.92	1.17	0.91	2.05	0.14	1.71	1.73	1.94
B97-2	-3.13	3.52	-1.43	1.47	0.62	1.91	-3.09	3.24	2.54	1.96
PW6B95	-5.36	5.36	-2.05	2.05	-0.76	1.43	-3.14	3.14	2.99	2.04
B98	-5.18	5.18	-2.96	2.96	-0.31	1.97	-4.16	4.16	3.57	2.41
mPW1PW91	-5.99	5.99	-1.81	1.94	-0.38	2.00	-3.54	3.55	3.37	2.44
PBE1KCIS	-7.07	7.07	-2.41	2.41	-0.78	1.91	-3.68	3.72	3.78	2.62
B97-1	-5.18	5.18	-3.21	3.21	-0.23	1.83	-4.40	4.40	3.65	2.63
PBE1PBE	-6.62	6.62	-1.87	2.05	-0.58	2.16	-4.22	4.22	3.76	2.75
B3LYP	-8.49	8.49	-3.25	3.25	-1.42	2.02	-4.13	4.23	4.50	3.08
MPW1KCIS	-8.64	8.64	-3.55	3.55	-1.21	1.96	-4.39	4.41	4.64	3.16
X3LYP	-8.48	8.48	-2.89	2.90	-1.43	2.06	-3.98	4.09	4.38	3.29
MPW3LYP	-9.29	9.29	-4.29	4.29	-1.61	2.21	-4.66	4.71	5.13	3.38
TPSS1KCIS	-9.26	9.26	-4.88	4.88	-1.39	2.12	-4.69	4.69	5.24	3.52
MP2	11.76	11.76	0.74	0.74	4.71	5.44	3.69	4.14	5.52	3.99
TPSSh	-11.51	11.51	-5.78	5.78	-2.94	3.23	-5.97	5.97	6.62	4.54
TPSSKCIS	-13.37	13.37	-7.64	7.64	-2.56	2.98	-7.01	7.01	7.75	5.00
BLYP	-14.66	14.66	-8.40	8.40	-3.38	3.51	-7.52	7.52	8.52	5.53
TPSS	-14.65	14.65	-7.75	7.75	-3.84	4.04	-7.71	7.71	8.54	5.68
PBE	-14.93	14.93	-6.97	6.97	-2.94	3.35	-9.32	9.32	8.64	5.89
SPWL	-23.48	23.48	-8.50	8.50	-5.17	5.90	-17.72	17.72	13.90	10.17

^a MUE denotes mean unsigned error (kcal/mol). MSE denotes mean signed error (kcal/mol). MMUE in this table is calculated by averaging the numbers in column 2, 4, 6, and 8. ^b AMUE is defined in as: $AMUE = [MUE(\Delta E, 38) + MMUE]/2$, where $MUE(\Delta E, 38)$ is the mean unsigned error for the energy of reactions for the 38 reactions involved in this table. AMUE is a measure of the quality of a method for kinetics. ^c The QCISD/MG3 geometries and MG3S basis set are used for calculations in this table. ^d NS denote nucleophilic substitution reactions. ^e This denote unimolecular and association reactions.

TABLE 6: Mean Errors for Nonbonded Databases (kcal/mol)^{a,b,c}

method	HB6/04			CT7/04			DI6/04			WI7/05			PPS5/05			
	MUE			MUE			MUE			MUE			MUE			
	no-cp	cp	MMUE	no-cp	cp	MMUE	MMMUE									
PWB6K	0.44	0.34	0.39	0.25	0.16	0.21	0.24	0.32	0.28	0.15	0.07	0.11	0.79	1.00	0.90	0.38
MP2	0.26	0.93	0.60	0.73	0.26	0.49	0.45	0.25	0.35	0.07	0.18	0.13	1.26	0.50	0.88	0.49
MPWB1K	0.41	0.70	0.56	0.24	0.45	0.34	0.50	0.65	0.57	0.08	0.16	0.12	1.32	1.57	1.45	0.61
PW6B95	0.53	0.78	0.65	0.69	0.47	0.58	0.40	0.49	0.45	0.11	0.09	0.10	1.21	1.44	1.32	0.62
MPW1B95	0.50	0.86	0.68	0.47	0.31	0.39	0.50	0.63	0.56	0.10	0.16	0.13	1.46	1.70	1.58	0.67
B97-1	0.45	0.45	0.45	1.17	0.89	1.03	0.28	0.30	0.29	0.10	0.11	0.10	1.57	1.78	1.68	0.71
PBE1PBE	0.40	0.28	0.34	1.04	0.75	0.90	0.35	0.38	0.37	0.12	0.18	0.15	1.84	2.09	1.96	0.74
PBE1KCIS	0.49	0.59	0.54	0.89	0.63	0.76	0.32	0.38	0.35	0.12	0.14	0.13	1.92	2.13	2.02	0.76
B98	0.45	0.66	0.55	0.91	0.66	0.79	0.34	0.40	0.37	0.12	0.16	0.14	1.91	2.13	2.02	0.78
MPW1K	0.33	0.61	0.47	0.44	0.66	0.55	0.52	0.67	0.60	0.20	0.29	0.25	2.25	2.53	2.39	0.85
MPW3LYP	0.51	0.41	0.46	1.39	1.06	1.22	0.31	0.36	0.34	0.19	0.16	0.18	2.11	2.34	2.22	0.88
X3LYP	0.45	0.48	0.47	0.96	0.68	0.82	0.45	0.59	0.52	0.16	0.22	0.19	2.49	2.71	2.60	0.92
mPW1PW91	0.39	0.79	0.59	0.65	0.51	0.58	0.53	0.63	0.58	0.58	0.30	0.44	2.43	2.71	2.57	0.95
TPSS1KCIS	0.49	0.86	0.67	1.22	0.95	1.08	0.46	0.55	0.50	0.17	0.21	0.19	2.39	2.62	2.50	0.99
MPWKICIS1K	0.59	1.00	0.80	0.52	0.85	0.69	0.75	0.90	0.83	0.18	0.25	0.22	2.56	2.80	2.68	1.04
TPSSh	0.41	0.80	0.60	1.44	1.16	1.30	0.49	0.58	0.54	0.18	0.26	0.22	2.46	2.72	2.59	1.05
MPW1KCIS	0.87	1.28	1.07	0.85	0.68	0.77	0.66	0.82	0.74	0.20	0.27	0.24	2.65	2.88	2.76	1.12
B3LYP	0.60	0.93	0.76	0.71	0.54	0.63	0.78	0.94	0.86	0.31	0.39	0.35	2.95	3.17	3.06	1.13
BB1K	0.99	1.37	1.18	0.68	1.00	0.84	1.02	1.16	1.09	0.34	0.44	0.39	2.03	2.27	2.15	1.13
PBE	0.45	0.32	0.39	2.95	2.63	2.79	0.46	0.40	0.43	0.13	0.15	0.14	1.86	2.09	1.97	1.14
TPSSKCIS	0.55	0.89	0.72	2.17	1.84	2.01	0.49	0.52	0.50	0.18	0.22	0.20	2.48	2.70	2.59	1.20
TPSS	0.45	0.82	0.63	2.20	1.86	2.03	0.52	0.56	0.54	0.19	0.26	0.22	2.53	2.78	2.66	1.22
B97-2	1.22	1.64	1.43	0.56	0.67	0.61	0.87	1.02	0.94	0.25	0.35	0.30	2.73	2.96	2.84	1.23
B1B95	1.31	1.69	1.50	0.53	0.72	0.62	1.11	1.26	1.19	0.42	0.51	0.47	2.34	2.58	2.46	1.25
BLYP	1.18	1.56	1.37	1.67	1.42	1.54	1.00	1.18	1.09	0.45	0.53	0.49	3.58	3.79	3.69	1.63
SPWL	4.64	4.20	4.42	6.78	6.41	6.59	2.93	2.73	2.83	0.30	0.20	0.25	0.35	0.43	0.39	2.90

^a MUE denotes mean unsigned error (MUE). MMUE = $[MUE(cp) + MUE(no-cp)]/2$, and MMMUE = $[MMUE(HB) + MMUE(CT) + MMUE(DI) + MMUE(WI) + MMUE(PPS)]/5$. HB: hydrogen bonding. CT: charge transfer. DI: dipole interaction. WI: weak interaction. PPS: π - π stacking. ^b We use "no-cp" to denote the calculation without the counterpoise correction for the BSSE, and use "cp" to denote the calculation with the counterpoise correction for the BSSE. ^c MC-QCISD/3 geometries and the MG3S basis set are used for calculations in this table.

interactions). Furthermore, it is known to sometimes overcorrect. Because this is a paper about practical DFT and not about cp,

we simply use the average in eq 21 without arguing one way or another about the merits of cp corrections. Those who prefer

TABLE 7: Mean Signed Errors for the Nonbonded Database^a

method	HB6/04		CT7/04		DI6/04		WI7/05		PPS5/05	
	no-cp	cp	no-cp	cp	no-cp	cp	no-cp	cp	no-cp	cp
PWB6K	0.17	-0.23	0.23	-0.09	-0.12	-0.26	0.15	0.07	-0.77	-0.78
MP2	0.24	-0.93	0.73	-0.21	0.45	-0.08	0.04	-0.18	1.26	1.22
MPWB1K	-0.31	-0.70	-0.12	-0.45	-0.50	-0.65	-0.06	-0.16	-1.32	-1.33
PW6B95	-0.39	-0.78	0.65	0.29	-0.34	-0.49	0.06	-0.03	-1.21	-1.22
MPW1B95	-0.46	-0.86	0.36	0.04	-0.48	-0.63	-0.06	-0.16	-1.46	-1.47
B97-1	-0.04	-0.43	1.17	0.86	0.09	-0.06	-0.01	-0.09	-1.57	-1.58
PBE1PBE	0.19	-0.23	1.04	0.71	0.03	-0.13	-0.09	-0.18	-1.84	-1.85
PBE1KCIS	-0.20	-0.59	0.87	0.56	-0.17	-0.32	-0.04	-0.12	-1.92	-1.92
B98	-0.26	-0.66	0.87	0.55	-0.17	-0.32	-0.07	-0.16	-1.91	-1.92
MPW1K	-0.17	-0.61	-0.21	-0.56	-0.51	-0.67	-0.19	-0.29	-2.25	-2.26
MPW3LYP	0.26	-0.14	1.39	1.06	-0.14	-0.30	0.05	-0.03	-2.11	-2.12
X3LYP	-0.05	-0.44	0.96	0.65	-0.43	-0.59	-0.14	-0.22	-2.49	-2.50
mPW1PW91	-0.36	-0.79	0.53	0.18	-0.46	-0.63	0.18	-0.30	-2.43	-2.44
TPSS1KCIS	-0.43	-0.86	1.18	0.85	-0.37	-0.53	-0.11	-0.21	-2.39	-2.40
MPWKIS1K	-0.59	-1.00	-0.52	-0.85	-0.75	-0.90	-0.15	-0.25	-2.56	-2.57
TPSSh	-0.36	-0.80	1.43	1.09	-0.38	-0.54	-0.16	-0.26	-2.46	-2.47
MPW1KCIS	-0.87	-1.28	0.70	0.37	-0.66	-0.82	-0.17	-0.26	-2.65	-2.65
B3LYP	-0.55	-0.93	0.61	0.30	-0.68	-0.94	-0.31	-0.39	-2.95	-2.96
BB1K	-0.99	-1.37	-0.68	-1.00	-1.02	-1.16	-0.34	-0.44	-2.03	-2.04
PBE	0.22	-0.19	2.95	2.63	0.38	0.20	-0.04	-0.12	-1.86	-1.86
TPSSKCIS	-0.46	-0.89	2.17	1.84	-0.26	-0.43	-0.10	-0.20	-2.48	-2.49
TPSS	-0.37	-0.82	2.20	1.86	-0.29	-0.46	-0.15	-0.25	-2.53	-2.54
B97-2	-1.22	-1.64	-0.10	-0.43	-0.87	-1.02	-0.25	-0.35	-2.73	-2.73
B1B95	-1.31	-1.69	-0.27	-0.59	-1.11	-1.26	-0.42	-0.51	-2.34	-2.35
BLYP	-1.18	-1.56	1.63	1.32	-1.00	-1.18	-0.45	-0.53	-3.58	-3.59
SPWL	3.13	2.67	5.61	5.23	2.16	1.95	0.30	0.20	0.23	0.22

^a MC-QCISD/3 geometries and the MG3S basis set are used for calculations in this table. ^b The order of the methods in this table is the same as that in Table 6. ^c MSE denotes mean signed error (MSE). ^d We use “no-cp” to denote the calculation without the counterpoise correction for the BSSE, and use “cp” to denote the calculation with the counterpoise correction for the BSSE.

a different approach can find the separate cp and no-cp values in our tables.

Table 6 shows that PBE1PBE, PBE, PWB6K, and B97-1 give the best performance for calculating the binding energies for the hydrogen bonding dimers in the HB6/04 database.

In 1996, Ruiz, Salahub, and Vela⁷⁸ reported that some GGA methods seriously overestimate the binding energies and geometries of some charge-transfer complexes. From Table 6 and Table 7, we can also see that the LSDA (SPWL), GGAs (BLYP, PBE), meta GGAs (TPSS, TPSSKCIS) give much larger MMUE and MSE than hybrid GGAs and hybrid meta GGAs. The wrong asymptotic behavior of the exchange and correlation functionals in DFT leads to a small energy gap between electron donor’s HOMO and the acceptor’s LUMO. The small gap leads to too much charge transfer and is the cause of the overestimation of the strength of the charge-transfer interaction. Inclusion of HF exchange in the DFT calculation can increase the HOMO–LUMO gap; hence hybrid functionals can give better performance,⁷⁹ as shown here by the low MMUE obtained by some hybrid and hybrid meta GGA methods such as PWB6K, MPWB1K, MPW1B95, and MPW1K. These methods give the best performance for calculating the binding energies of the charge transfer complexes, with the first three methods outperforming MP2. PW6B95 is only slightly worse than MPW1K.

Table 6 also shows that PWB6K, B97-1, MPW3LYP, and MP2 give the best performance for calculating the binding energies for the dipole interaction complexes in the DI6/04 database.

PWB6K, MP2, PW6B95, and B97-1 give the best performance for calculating the binding energies for the weak interaction complexes in the WI7/05 database. Note that PWB6K outperforms the MP2 method for all of the above four types of nonbonded interactions; this is encouraging because PWB6K is computationally much less expensive than MP2, and it

therefore has broader applicability in biological and recognition systems where nonbonded interactions are important. Of course, just as empirical parameters may be used to improve the performance of DFT for nonbonded interactions such as dispersion interactions, empirical procedures may also be able to improve wave function methods such as MP2, configuration interaction theory, and coupled-cluster theory for dispersion and other interactions,^{80–85} but discussion of such methods is beyond the scope of the present article.

It is well-known that MP2 has the correct asymptotic R^{-6} binding behavior (where R is the internuclear distance for rare gas dimers), but DFT with the functional studied here does not have this property. In Figure 2, we compare the calculated potential energy curve of the Ar₂ dimer by PWB6K and MP2 with the 6-311+G(2df,2p) basis set, and we also present the curve for $-C_6 \times R^{-6}$, where C_6 is the accurate value taken from literature.^{86,87} The first observation from Figure 2 is that the counterpoise correction has a stronger effect for MP2 than for PWB6K. The MP2-nocp curve deviates from the MP2-cp curve much more than the PWB6K method does. The D_e by MP2-cp is 0.11 kcal/mol which is 50% less than that by MP2-nocp, whereas the D_e by PWB6K-cp is 0.25 kcal/mol which is only 8% less than that by PWB6K-nocp. Note that the experimental D_e is 0.28 kcal/mol, so the Ar₂ test case is consistent with the conclusion we drew from Table 6 and Table 7 that PWB6K outperforms MP2 for the dispersion interactions. Figure 2 and Table S8 in the Supporting Information also show that near the bottom of the van der Waals well, neither PWB6K nor MP2 gives a curve parallel to the R^{-6} curve. When intermolecular distance R increases to 6 Å, MP2 begins to approach the correct R^{-6} asymptotic form, whereas the PWB6K method does not have this asymptotic behavior. However, at 6 Å the interaction energy for Ar₂ is only 2×10^{-2} kcal/mol, so the fact that DFT has the wrong asymptotic behavior is not significant for many problems. (However, it would be significant

TABLE 8: Predicted Binding Energies (kcal/mol) for Eight of the Cases in the Nonbonded Interactions Databases As Calculated with MG3S Basis Set at MC-QCISD/3 Geometries

method	HeNe	HeAr	NeAr	(CH ₄) ₂	(HCl) ₂	(H ₂ O) ₂	(C ₂ H ₄) ₂ ···F ₂	(C ₆ H ₆)-PD
Without Counterpoise Corrections								
PW6B95	0.15	0.14	0.22	0.32	1.61	5.12	1.64	0.81
B97-1	0.09	0.11	0.22	0.19	1.97	5.33	1.86	-0.01
PWB6K	0.16	0.19	0.28	0.56	1.80	5.51	1.31	1.35
MPW1B95	0.09	0.07	0.11	0.12	1.46	4.99	1.30	0.50
B98	0.07	0.08	0.18	0.02	1.76	5.16	1.63	-0.48
B3LYP	-0.03	-0.07	0.01	-0.51	1.32	4.96	1.50	-1.97
MP2	0.05	0.05	0.20	0.40	2.23	5.46	1.59	5.31
accurate ^b	0.04	0.06	0.13	0.52	2.01	4.97	1.07	2.78
With Counterpoise Corrections								
PW6B95	0.12	0.13	0.14	0.30	1.47	4.69	1.35	0.39
B97-1	0.07	0.09	0.13	0.18	1.82	4.91	1.57	-0.41
PWB6K	0.14	0.17	0.20	0.55	1.68	5.09	1.01	0.91
MPW1B95	0.06	0.06	0.03	0.10	1.32	4.56	0.99	0.05
B98	0.05	0.06	0.09	0.01	1.60	4.72	1.33	-0.91
MP2	-0.01	0.02	0.00	0.29	1.80	4.53	0.92	3.77
accurate ^b	0.04	0.06	0.13	0.52	2.01	4.97	1.07	2.78

^a This is the parallel displaced benzene dimer. ^b Accurate values from the database.

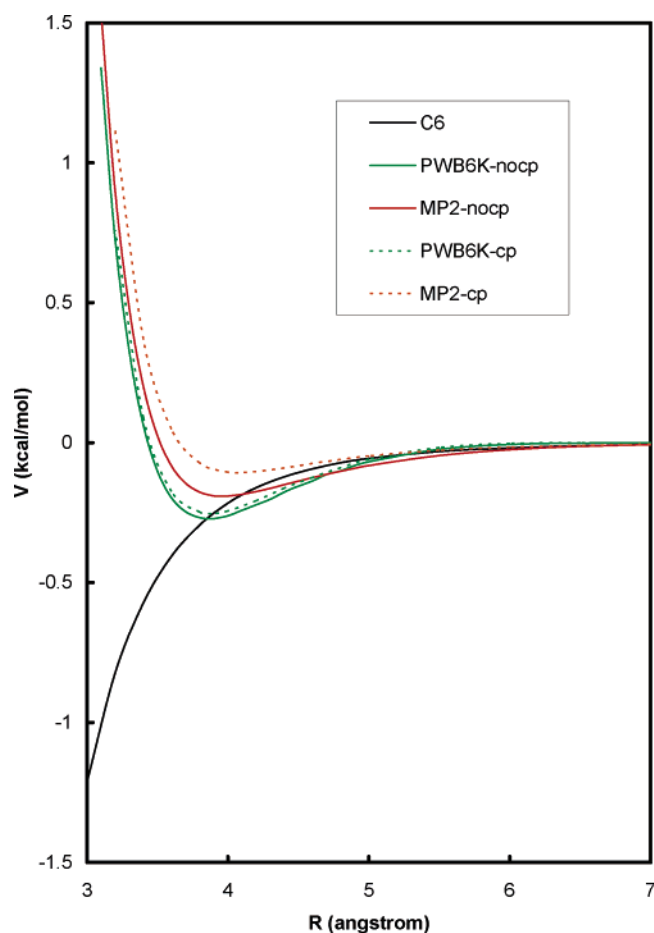


Figure 2. Potential energy curves for the Ar₂ dimer. The curve labeled “C6” is $-C_6R^{-6}$ with the C_6 coefficient for Ar₂ taken from literature.^{86,87} The curves labeled “no-cp” denote calculations without the counterpoise correction for the BSSE, and the curves labeled “cp” denote calculations that include the counterpoise correction. The basis set used for all calculations in this figure is 6-311+G(2df,2p). The equilibrium dissociation energies D_e corresponding to the various curves (in kcal/mol) are 0.19 (MP2-nocp), 0.11 (MP2-cp), 0.27 (PWB6K-nocp), and 0.25 (PWB6K-cp); these values may be compared to 0.28 from experiment.⁹⁰ The equilibrium bond lengths R_e (in Å) corresponding to the various curves are 3.96 (MP2-nocp), 4.07 (MP2-cp), 3.88 (PWB6K-nocp and PWB6K-cp); these values may be compared to 3.76 from experiment.⁹⁰

for low-energy, small-angle differential cross sections^{88,89} for elastic scattering.)

Table 8 compares the prediction of six density functional methods to MP2 for the binding energies of HeNe, HeAr, NeAr, and (CH₄)₂ and four of the stronger nonbonded interactions. Table 8 is presented to illustrate the overall trends in the predictions by considering some specific examples.

π - π stacking interactions play a dominant role in stabilizing various biopolymers, for example, the double helix structure of DNA, and such interaction are also important for supramolecular design. Tables 6 and 7 show that the quality of PWB6K for describing π - π stacking interactions is comparable to MP2, although PWB6K and most DFT methods underestimate the strength of π - π stacking interactions, whereas MP2 overestimates the binding energies. Surprisingly and interestingly, the LSDA (SPWL) gives the best performance for π - π stacking, but this is apparently due largely to error cancellation because LSDA seriously overestimates covalent interactions and other types of weak interactions.

We also define the mean MMUE as

$$\text{MMMUE} = [\text{MMUE}(\text{HB}) + \text{MMUE}(\text{CT}) + \text{MMUE}(\text{DI}) + \text{MMUE}(\text{WI}) + \text{MMUE}(\text{PPS})]/5 \quad (22)$$

If we use MMMUE as a criterion to evaluate the overall performance of DFT methods and MP2 for nonbonded interactions, we can see from Table 6 that the performance of PWB6K, MP2, MPWB1K, and PW6B95 are the best, followed by MPW1B95, PBE1PBE, B97-1, and MPW1K.

4.4. Overall Results. Table 9 is a summary of the performance of the tested methods for all quantities studied in this paper. The TCAE (thermochemical average error) is defined as

$$\text{TCAE} = (\text{TMUE} \times 2 + \text{MMMUE})/3 \quad (23)$$

where TMUE is from Table 4 and MMMUE is from Table 6, and this is the final measure that we use for the quality of a method for thermochemistry. The factor of 2 is included because in this average we want to emphasize the performance for the thermochemistry database. The TKAE (thermochemical kinetics average error) in Table 9 is defined as

$$\text{TKAE} = (\text{AMUE} \times 2 + \text{MMMUE})/3 \quad (24)$$

where the AMUE is from Table 5, and again MMMUE is from Table 6. TKAE is the final measure that we use for the quality of a method for thermochemical kinetics. Clearly the exact

TABLE 9: Overall Results^{a,b}

method	thermochemistry	kinetics	nonbonded	TCAE ^b	TKAE ^c
	TMUE	AMUE	interaction MMMUE		
PWB6K	1.72	1.59	0.38	1.27	1.18
MPWB1K	1.38	1.60	0.61	1.12	1.27
BB1K	1.70	1.50	1.13	1.51	1.38
MPW1K	2.59	1.82	0.85	2.01	1.49
MPW1B95	0.98	1.92	0.67	0.88	1.50
PW6B95	0.81	2.04	0.62	0.74	1.57
B1B95	0.96	1.78	1.25	1.05	1.60
MPWKCIS1K	2.92	1.94	1.04	2.29	1.64
B97-2	1.02	1.96	1.23	1.09	1.72
B98	1.00	2.41	0.78	0.93	1.87
mPW1PW91	1.32	2.44	0.95	1.20	1.94
B97-1	1.07	2.63	0.71	0.95	1.99
PBE1KCIS	1.36	2.62	0.76	1.16	2.00
PBE1PBE	1.31	2.75	0.74	1.12	2.08
B3LYP	1.41	3.08	1.13	1.32	2.43
MPW1KCIS	1.34	3.16	1.12	1.27	2.48
X3LYP	1.89	3.29	0.92	1.57	2.50
MPW3LYP	1.13	3.38	0.88	1.05	2.55
TPSS1KCIS	1.07	3.52	0.99	1.04	2.68
MP2	2.28	3.99	0.49	1.68	2.82
TPSSh	1.37	4.54	1.05	1.26	3.38
TPSSKCIS	1.40	5.00	1.20	1.33	3.73
TPSS	1.36	5.68	1.22	1.31	4.19
BLYP	1.93	5.53	1.63	1.83	4.23
PBE	3.01	5.89	1.14	2.39	4.31
SPWL	14.70	10.17	2.90	10.76	7.75

^a TMUE for thermochemistry is from Table 4, AMUE for kinetics is from Table 5, and the MMMUE for nonbonded interaction is from Table 6. ^b TCAE = (TMUE × 2 + MMMUE)/3. ^c TKAE = (AMUE × 2 + MMMUE)/3.

position in Table 8 is not as meaningful as the general trends, but the table provides a way to organize the discussion. As in other tables, the five smallest average errors for each of the individual quantities are in bold, except for the final column, where the 10 best methods are bold.

Using thermochemical average error (TCAE) in Table 9 as the overall, summarizing measure of quality of the tested methods for thermochemistry, we can see that PW6B95 is the best method, followed by MPW1B95, B98, B97-1, and TPSS1KCIS.

Using thermochemical kinetics average error (TKAE) in Table 9 as the overall, summarizing measure of quality of tested methods for thermochemical kinetics, we can see that PWB6K, MPWB1K, BB1K, MPW1K, and MPW1B95 are the best of all the tested methods for thermochemical kinetics.

Note that all the conclusions in Table 9 were drawn on the basis of calculations with the MG3S basis, which is a multiply polarized, augmented valence-triple- ζ basis including core-

polarizing d functions for P, S, and Cl. We also did some calculations with the 6-31+G(d,p) basis set, and the conclusions based on the calculations with this polarized and augmented double- ζ basis set are similar to the above conclusions. Finally we explored the performance of the B3LYP, MPW1B95, and PW6B95 methods for the calculation of atomization energies, hydrogen transfer reaction barrier heights, ionization potentials and electron affinities with a third basis set, namely, the 6-311++G(3df,3pd) basis set^{65,66} (we denote this basis as triply polarized triple- ζ (TPTZ) in Table 10), and the results are summarized in Table 10. Table 10 shows that PW6B95 is the best for all three basis sets, although it was optimized by using the 6-31+G(d,p) basis set. Note that MPW1B95 works better with the MG3S basis set than with the 6-311++G(3df,3pd) basis set, whereas B3LYP works better with the 6-311++G(3df,-3pd) basis set than with the MG3S basis set.

4.5. Concluding Remarks. This paper developed two new hybrid meta exchange-correlation functionals for thermochemistry, thermochemical kinetics, and nonbonded interactions in main group atoms and molecules. The resulting methods were comparatively assessed against the MGAE109/3 main group atomization energy database, against the IP13/3 ionization potential database, against the EA13/3 electron affinity database, against the HTBH38/4 and NHTBH38/04 barrier height database, against the HB6/04 hydrogen bonding database, against the CT7/04 charge-transfer database, against the DI6/04 dipole interaction database, against the WI7/05 weak interaction database and against the PPS5/05 π - π stacking database. From the above assessment and comparison, we draw the following conclusions, based on an analysis of mean unsigned errors:

(1) The PW6B95, MPW1B95, B98, B97-1 and TPSS1KCIS functionals give the best results for a combination of thermochemistry and nonbonded interactions.

(2) The PWB6K, MPWB1K, BB1K, MPW1K, and MPW1B95 functionals give the best results for a combination of thermochemical kinetics and nonbonded interactions.

(3) The new PWB6K functional is the first functional to outperform the MP2 method for nonbonded interactions.

(4) PW6B95 gives errors for main group covalent bond energies that are only 0.41 kcal (as measured by MUEPB for the MGAE109 database), as compared to 0.56 kcal/mol for the second best method and 0.92 kcal/mol for B3LYP.

From the present study, we recommend PW6B95, MPW1B95, B98, B97-1, and TPSS1KCIS for general purpose applications in thermochemistry and we recommend PWB6K, MPWB1K, BB1K, MPW1K, and MPW1B95 for kinetics. It is very encouraging that we succeeded in developing density functionals

TABLE 10: Comparison of the Effect of Basis Set for the Performance of the PW6B95, MPW1B95, and B3LYP Methods for Calculating Atomization Energies, Hydrogen Transfer Reaction Barrier Heights, Ionization Potentials, and Electron Affinities^a

item	PW6B95			MPW1B95			B3LYP			
	DIDZ ^c	MG3S	TPTZ ^c	DIDZ ^c	MG3S	TPTZ ^c	DIDZ ^c	MG3S	TPTZ ^c	
MUE	atomization energies (109)	4.62	1.88	2.19	4.74	2.91	3.55	8.04	4.28	3.70
	HCO compounds (54)	2.31	1.68	1.92	4.07	3.01	3.46	4.70	3.19	2.64
	containing second row atom (34)	8.49	2.26	2.37	6.86	2.53	3.27	13.60	6.45	5.84
	other (21)	4.30	1.79	2.60	3.05	3.26	4.24	7.65	3.55	2.97
MUEPB ^b	error per bond (109)	0.98	0.40	0.47	1.01	0.62	0.75	1.71	0.91	0.79
	HCO compounds (54)	0.37	0.27	0.31	0.65	0.48	0.55	0.75	0.51	0.42
	containing second row atom (34)	3.04	0.81	0.85	2.46	0.91	1.17	4.88	2.31	2.09
	other (21)	1.11	0.46	0.67	0.79	0.85	1.10	1.98	0.92	0.77
MUE	HT reaction barrier heights (38)	3.51	3.14	3.33	3.68	3.02	3.22	4.69	4.23	4.41
MUE	ionization potentials (13)	3.48	3.24	3.24	2.40	2.14	2.12	4.91	4.72	4.69
MUE	electron affinities (13)	2.03	1.78	1.78	2.99	2.91	2.97	3.24	2.29	2.27

^a QCISD/MG3 geometries are used for calculations in this table. ^b MUEPB denotes mean unsigned error (MUE) per bond. ^c TPTZ denotes the 6-311++G(3df,3pd) basis set, and DIDZ denotes the 6-31+G(d,p) basis.

with very broad applicability. They should be especially useful for kinetics and for condensed-phase systems and molecular recognition problems (including supramolecular chemistry and protein assemblies) where nonbonded interactions are very important.

Acknowledgment. We are grateful to Erin Dahlke and Benjamin Lynch for helpful suggestions. This work was supported in part by the U.S. Department of Energy, Office of Basic Energy Sciences.

Supporting Information Available: The training sets and all the databases are given in the Supporting Information. The mean signed errors for nonbonded interactions are also given in the Supporting Information. This material is available free of charge via the Internet at <http://pubs.acs.org>.

References and Notes

- Perdew, J. P.; Zunger, A. *Phys. Rev. B* **1981**, *23*, 5048.
- Perdew, J. P. *Phys. Rev. B* **1986**, *33*, 8822.
- Becke, A. D. *Phys. Rev. A* **1988**, *38*, 3098.
- Lee, C.; Yang, W.; Parr, R. G. *Phys. Rev. B* **1988**, *37*, 785.
- Perdew, J. P. In *Electronic Structure of Solids '91*; Ziesche, P., Eschig, H., Eds.; Akademie Verlag: Berlin, 1991; p 11.
- Perdew, J. P.; Wang, Y. *Phys. Rev. B* **1992**, *45*, 13244.
- Becke, A. D. *J. Chem. Phys.* **1993**, *98*, 1372.
- Becke, A. D. *J. Chem. Phys.* **1993**, *98*, 5648.
- Stephens, P. J.; Devlin, F. J.; Chabalowski, C. F.; Frisch, M. J. *J. Phys. Chem.* **1994**, *98*, 11623.
- Becke, A. D. *J. Chem. Phys.* **1996**, *104*, 1040.
- Perdew, J. P.; Burke, K.; Ernzerhof, M. *Phys. Rev. Lett* **1996**, *77*, 3865.
- Perdew, J. P.; Ernzerhof, M.; Burke, K. *J. Chem. Phys.* **1996**, *105*, 9982.
- Becke, A. D. *J. Chem. Phys.* **1997**, *107*, 8554.
- Adamo, C.; Barone, V. *J. Chem. Phys.* **1998**, *108*, 664.
- Schmidler, H. L.; Becke, A. D. *J. Chem. Phys.* **1998**, *108*, 9624.
- Voorhis, T. V.; Scuseria, G. E. *J. Chem. Phys.* **1998**, *109*, 400.
- Hamprecht, F. A.; Cohen, A. J.; Tozer, D. J.; Handy, N. C. *J. Chem. Phys.* **1998**, *109*, 6264.
- Handy, N. C.; Tozer, D. J. *Mol. Phys.* **1998**, *94*, 707.
- Krieger, J. B.; Chen, J.; Iafate, G. J. *Int. J. Quantum Chem.* **1998**, *69*, 255.
- Rey, J.; Savin, A. *Int. J. Quantum Chem.* **1998**, *69*, 581.
- Krieger, J. B.; Chen, J.; Iafate, G. J.; Savin, A. In *Electron Correlations and Materials Properties*; Gonis, A., Kioussis, N., Eds.; Plenum: New York, 1999; p 463.
- Engel, E.; Dreizler, R. M. *J. Comput. Chem.* **1999**, *20*, 31.
- Perdew, J. P.; Kurth, S.; Zupan, A.; Blaha, P. *Phys. Rev. Lett* **1999**, *82*, 2544.
- Becke, A. D. *J. Chem. Phys.* **2000**, *112*, 4020.
- Lynch, B. J.; Fast, P. L.; Harris, M.; Truhlar, D. G. *J. Phys. Chem. A* **2000**, *104*, 4811.
- Proynov, E.; Chermette, H.; Salahub, D. R. *J. Chem. Phys.* **2000**, *113*, 10013.
- Handy, N. C.; Cohen, A. J. *Mol. Phys.* **2001**, *99*, 403.
- Perdew, J. P.; Schmidt, K. In *Density Functional Theory and Its Applications to Materials*; Doren, V., Alsenoy, C. V., Geerlings, P., Eds.; American Institute of Physics: New York, 2001.
- Lynch, B. J.; Truhlar, D. G. *J. Phys. Chem. A* **2001**, *105*, 2936.
- Wilson, P. J.; Bradley, T. J.; Tozer, D. J. *J. Chem. Phys.* **2001**, *115*, 9233.
- Adamo, C.; Barone, V. *J. Chem. Phys.* **2002**, *116*, 5933.
- Boese, A. D.; Handy, N. C. *J. Chem. Phys.* **2002**, *116*, 9559.
- Baker, J.; Pulay, P. *J. Chem. Phys.* **2002**, *117*, 1441.
- Toulouse, J.; Savin, A.; Adamo, C. *J. Chem. Phys.* **2002**, *117*, 10465.
- Mattsson, A. E. *Science* **2002**, *298*, 759.
- Boese, A. D.; Martin, J. M. L.; Handy, N. C. *J. Chem. Phys.* **2003**, *119*, 3005.
- Boese, A. D.; Chandra, A.; Martin, J. M. L.; Marx, D. *J. Chem. Phys.* **2003**, *119*, 5965.
- Staroverov, V. N.; Scuseria, G. E.; Tao, J.; Perdew, J. P. *J. Chem. Phys.* **2003**, *119*, 12129.
- Tao, J.; Perdew, J. P.; Staroverov, V. N.; Scuseria, G. E. *Phys. Rev. Lett.* **2003**, *91*, 146401.
- Xu, X.; Goddard, W. A. *Proc. Natl. Acad. Sci. U.S.A.* **2004**, *101*, 2673.
- Perdew, J. P.; Tao, J.; Staroverov, V. N.; Scuseria, G. E. *J. Chem. Phys.* **2004**, *120*, 6898.
- Zhao, Y.; Pu, J.; Lynch, B. J.; Truhlar, D. G. *Phys. Chem. Chem. Phys.* **2004**, *6*, 673.
- Zhao, Y.; Lynch, B. J.; Truhlar, D. G. *J. Phys. Chem. A* **2004**, *108*, 2715.
- Zhao, Y.; Truhlar, D. G. *J. Phys. Chem. A* **2004**, *108*, 6908.
- Andersson, S.; Gruning, M. *J. Phys. Chem. A* **2004**, *108*, 7621.
- Boese, A. D.; Martin, J. M. L. *J. Chem. Phys.* **2004**, *121*, 3405.
- Xu, X.; William A. Goddard, I. *J. Chem. Phys.* **2004**, *121*, 4086.
- Zhao, Y.; Lynch, B. J.; Truhlar, D. G. *Phys. Chem. Chem. Phys.* **2005**, *7*, 43.
- Zhao, Y.; González-García, N.; Truhlar, D. G. *J. Phys. Chem. A* **2005**, *109*, 2012.
- Zhao, Y.; Truhlar, D. G. *J. Comput. Theory Comput.* **2005**, *1*, 415.
- Zhao, Y.; Truhlar, D. G. *J. Phys. Chem. A* **2004**, *108*, 6908.
- Wu, Q.; Yang, W. *J. Chem. Phys.* **2002**, *116*, 515.
- Grimme, S. *J. Comput. Chem.* **2004**, *25*, 1463.
- Walsh, T. R. *Phys. Chem. Chem. Phys.* **2005**, *7*, 443.
- Lynch, B. J.; Truhlar, D. G. *J. Phys. Chem. A* **2003**, *107*, 8996.
- Lynch, B. J.; Zhao, Y.; Truhlar, D. G. *J. Phys. Chem. A* **2003**, *107*, 1384.
- Lynch, B. J.; Truhlar, D. G. *J. Phys. Chem. A* **2003**, *107*, 3898.
- Curtiss, L. A.; Raghavachari, K.; Redfern, P. C.; Rassolov, V.; Pople, J. A. *J. Chem. Phys.* **1998**, *109*, 7764.
- Martin, J. M. L.; Oliveira, G. d. J. *J. Chem. Phys.* **1999**, *111*, 1843.
- Sinnokrot, M. O.; Valeev, E. F.; Sherrill, C. D. *J. Am. Chem. Soc.* **2002**, *124*, 10887.
- Lynch, B. J.; Zhao, Y.; Truhlar, D. G. <http://comp.chem.umn.edu/database>.
- Pople, J. A.; Head-Gordon, M.; Raghavachari, K. *J. Chem. Phys.* **1987**, *87*, 5968.
- Fast, P. L.; Sanchez, M. L.; Truhlar, D. G. *Chem. Phys. Lett.* **1999**, *306*, 407.
- Curtiss, L. A.; Redfern, P. C.; Raghavachari, K.; Rassolov, V.; Pople, J. A. *J. Chem. Phys.* **1999**, *110*, 4703.
- Frisch, M. J.; Pople, J. A.; Binkley, J. S. *J. Chem. Phys.* **1984**, *80*, 3265.
- Hehre, W. J.; Radom, L.; Schleyer, P. v. R.; Pople, J. A. *Ab Initio Molecular Orbital Theory*; Wiley: New York, 1986.
- Fast, P. L.; Truhlar, D. G. *J. Phys. Chem. A* **2000**, *104*, 6111.
- Sinnokrot, M. O.; Sherrill, C. D. *J. Phys. Chem. A* **2004**, *108*, 10200.
- Boys, S. F.; Bernardi, F. *Mol. Phys.* **1970**, *19*, 553.
- Schwenke, D. W.; Truhlar, D. G. *J. Chem. Phys.* **1985**, *82*, 2418.
- Frisch, M. J.; Trucks, G. W.; Schlegel, H. B.; Scuseria, G. E.; Robb, M. A.; Cheeseman, J. R.; Montgomery, J. A., Jr.; T. V.; Kudin, K. N.; Burant, J. C.; Millam, J. M.; Iyengar, S. S.; Tomasi, J.; Barone, V.; Mennucci, B.; Cossi, M.; Scalmani, G.; Rega, N.; Petersson, G. A.; Nakatsuji, H.; Hada, M.; Ehara, M.; Toyota, K.; Fukuda, R.; Hasegawa, J.; Ishida, M.; Nakajima, T.; Honda, Y.; Kitao, O.; Nakai, H.; Klene, M.; Li, X.; Knox, J. E.; Hratchian, H. P.; Cross, J. B.; Adamo, C.; Jaramillo, J.; Gomperts, R.; Stratmann, R. E.; Yazyev, O.; Austin, A. J.; Cammi, R.; Pomelli, C.; Ochterski, J. W.; Ayala, P. Y.; Morokuma, K.; Voth, G. A.; Salvador, P.; Dannenberg, J. J.; Zakrzewski, G.; Dapprich, S.; Daniels, A. D.; Strain, M. C.; Farkas, O.; Malick, D. K.; Rabuck, A. D.; Raghavachari, K.; Foresman, J. B.; Ortiz, J. V.; Cui, Q.; Baboul, A. G.; Clifford, S.; Cioslowski, J.; Stefanov, B. B.; Liu, G.; Liashenko, A.; Piskorz, P.; Komaromi, I.; Martin, R. L.; Fox, D. J.; Keith, T.; Al-Laham, M. A.; Peng, C. Y.; Nanayakkara, A.; Challacombe, M.; Gill, P. M. W.; Johnson, B.; Chen, W.; Wong, M. W.; Gonzalez, C.; Pople, J. A. *Gaussian 03*, Revision C.01; Gaussian, Inc.: Pittsburgh, PA, 2003.
- Stoll, H.; Pavlidou, C. M. E.; Preuss, H. *Theor. Chim. Acta* **1978**, *49*, 143.
- von-Weizsäcker, C. F. *Z. Phys.* **1935**, *96*, 431.
- Dirac, P. A. M. *Proc. Cambridge Philos. Soc.* **1930**, *26*, 376.
- Slater, J. C. *Quantum Theory of Matter*, 2nd ed.; McGraw-Hill: New York, 1968.
- Slater, J. C. *Quantum Theory of Molecular and Solids. Vol. 4: The Self-Consistent Field for Molecular and Solids*; McGraw-Hill: New York, 1974.
- Møller, C.; Plesset, M. S. *Phys. Rev.* **1934**, *46*, 618.
- Ruiz, E.; Salahub, D. R.; Vela, A. *J. Phys. Chem.* **1996**, *100*, 12265.
- Ruiz, E.; Salahub, D. R.; Vela, A. *J. Am. Chem. Soc.* **1995**, *117*, 1141.
- Brown, F.; Truhlar, D. G. *Chem. Phys. Lett.* **1985**, *117*, 307.
- Gordon, M. S.; Truhlar, D. G. *J. Am. Chem. Soc.* **1986**, *108*, 2.
- Giese, T. J.; York, D. M. *J. Chem. Phys.* **2004**, *120*, 590.
- Zhao, Y.; Lynch, B. J.; Truhlar, D. G. *J. Phys. Chem. A* **2004**, *108*, 4786.
- Subotnik, J. E.; Shao, Y.; Liang, W.; Head-Gordon, M. *J. Chem. Phys.* **2004**, *121*, 9220.
- Subotnik, J. E.; Head-Gordon, M. *J. Chem. Phys.* **2005**, *122*, 034109.

- (86) Kumar, A.; Meath, W. J. *Mol. Phys.* **1985**, *54*, 823.
(87) Cybulski, S. M.; Haley, T. P. *J. Chem. Phys.* **2004**, *121*, 7711.
(88) Parson, J. M.; Schafer, T. P.; Tully, F. P.; Siska, P. E.; Wong, Y. C.; Lee, Y.-T. *J. Chem. Phys.* **1970**, *53*, 2134.
(89) Parson, J. M.; Schafer, T. P.; Siska, P. E.; Tully, F. P.; Wong, Y. C.; Lee, Y.-T. *J. Chem. Phys.* **1970**, *53*, 3755.
(90) Ogilvie, J. F.; Wang, F. Y. H. *J. Mol. Struct.* **1992**, *273*, 277.